

Dual Internal Standards with Metals and Molecules for MALDI Imaging of Kidney

Lipids

Sarah Aboulmagd¹, Diego Esteban-Fernández^{1†}, Estefanía Moreno-Gordaliza^{2†}, Boris Neumann^{3,4}, A.H. El-Khatib^{1,5}, Alberto Lázaro⁶, Alberto Tejedor⁶, M. Milagros Gómez-Gómez², Michael W. Linscheid^{1*}.

¹Department of Chemistry, Humboldt-Universität zu Berlin, Brook-Taylor Str. 2, 12489 Berlin, Germany

²Department of Analytical Chemistry, Faculty of Chemistry, Universidad Complutense de Madrid, Avda. Complutense s/n, 28040, Madrid, Spain

³Proteome Factory, Magnusstraße 11, 12489 Berlin, Germany

⁴Charité-Universitätmedizin Berlin, Institute of Pharmacology, Hessische Straße 3-4, 10115 Berlin, Germany

⁵Pharmaceutical Analytical Chemistry Department, Faculty of pharmacy, Ain Shams University, Cairo, Egypt

⁶Renal Pathophysiology Laboratory, Department of Nephrology, Instituto de Investigación Sanitaria Gregorio Marañón, Hospital General Universitario Gregorio Marañón, C/ Dr. Esquerdo 46, 28007, Madrid, Spain

[†]Equal authors contribution

*Corresponding author: Michael W. Linscheid. michael.linscheid@chemie.hu-berlin.de. Phone +49 (0)30 2093 7588; Fax +49 (0)30 2093 6985

Supporting Information

Table of contents

Direct infusion and laser ablation ICP-MS analysis

Direct infusion ICP-MS

LA-ICP-MS

Table S1

Figures S1 to S15

Direct injection and laser ablation ICP-MS analysis

Nitrocellulose membranes (NC) (Whatman® Protran® nitrocellulose membranes, Dassel, Germany) of approximately 10x10 mm were fixed to glass slides next to the tissue sections and printed simultaneously. The printed membranes were collected and used for direct infusion ICP-MS as well as LA-ICP-MS.

Direct infusion ICP-MS

The collected NC membranes were weighed and digested in 150 µL 69% HNO₃ (HNO₃, ultraquality, Carl Roth, Germany) for direct injection ICP-MS analysis. Digested samples were diluted in a ratio of 1:10 in 3.5% HNO₃ including 10 µL ¹⁴¹Pr (100 µg L⁻¹) as internal standard to a final volume of 500 µL. For external calibration, a solution series from 20 ng L⁻¹ to 10 µg L⁻¹ using ¹⁶⁹Tm standard solution was prepared. The Element XR sector field ICP-MS (Thermo Fisher Scientific, Bremen, Germany) was connected to a Meinhard-type nebulizer with a cyclonic spray chamber (MicroMist, Glass Expansion, Melbourne, Australia) using a nebulizer gas flow rate of 1.0 L min⁻¹ Ar. The instrument was operated at plasma gas flow of 15 L min⁻¹, auxiliary gas flow of 1.00 L min⁻¹, and RF plasma power of 1250 W.

LA-ICP-MS

LA-ICP-MS analysis was performed on a commercial LA system (UP-213, ESI, Portland, USA) coupled to a sector field ICP-MS (Element XR, Thermo Fisher Scientific, Bremen, Germany). The ICP-MS was synchronized using the LA unit in an external trigger mode. The operating conditions are shown in Table S1. The ICP-MS operating conditions were tuned daily for maximum intensity and low oxide ratio ((ThO/Th) < 0.7%) using a reference glass slide (SRM 612, NIST, Maryland USA). The printed nitrocellulose membranes were ablated continuously in line scans. Overlapping line scans and high laser shot repetition rates were applied to ensure complete ablation of the membrane sample.

Mass traces of ¹⁶⁹Tm were recorded at low resolution (R=300). The analysis of a nitrocellulose membrane (with 2x2 mm average dimensions) required about 20 min. Data was exported to Origin 2016 (OriginLab Corporation, Northampton, MA) where data normalization and generation of color coded images were performed.

Table S1. Instrumental parameters of the LA-ICP-MS measurements

ICP-MS		LA system	
RF plasma power	1257 W	Wavelength	213 nm
Plasma gas flow (Ar)	15 L min ⁻¹	Helium gas flow	0.8 L min ⁻¹
Sample gas flow (Ar)	1.3 L min ⁻¹	Laser energy	100% (5.16 J cm ⁻²)
Auxiliary gas flow (Ar)	0.99 L min ⁻¹	Laser spot size	100 µm
Mass resolution ($m/\Delta m$)	300 (LR)	Scan speed	100 µm s ⁻¹
Sample time	2 ms	Repetition rate	20 Hz
Scanning mode	E scan	Line overlapping	20%
Detected isotope	¹⁶⁹ Tm		

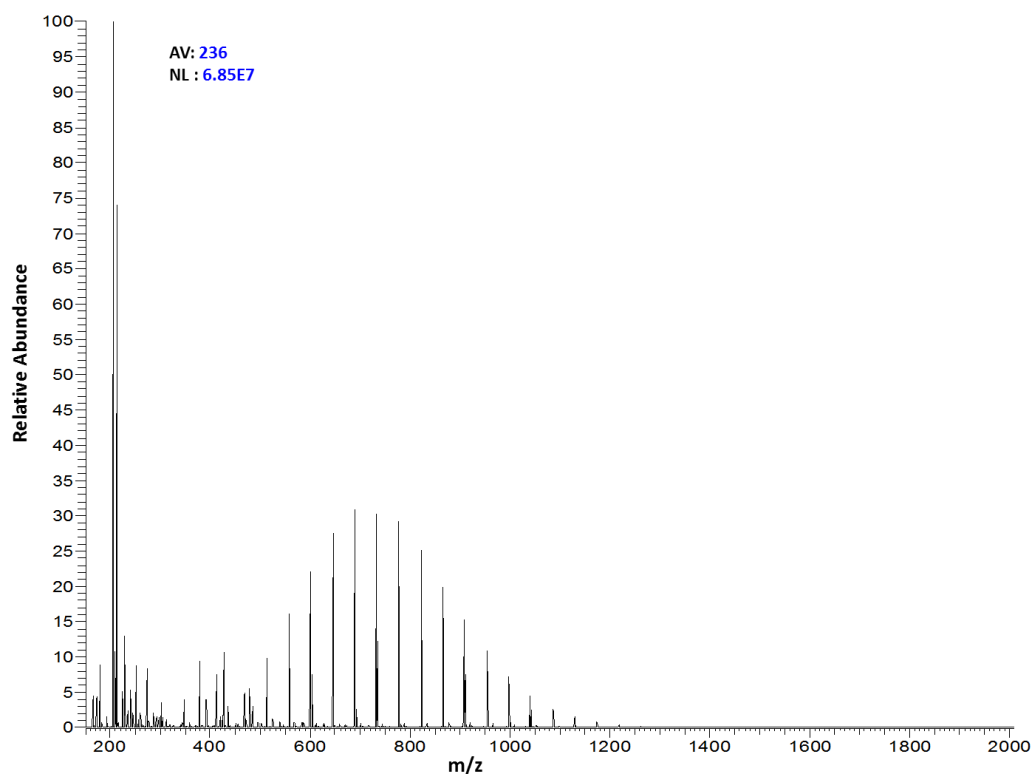


Figure S1. Mass spectrum showing background effect produced when colorless and yellow ink were used to dissolve DHB and the internal standards.

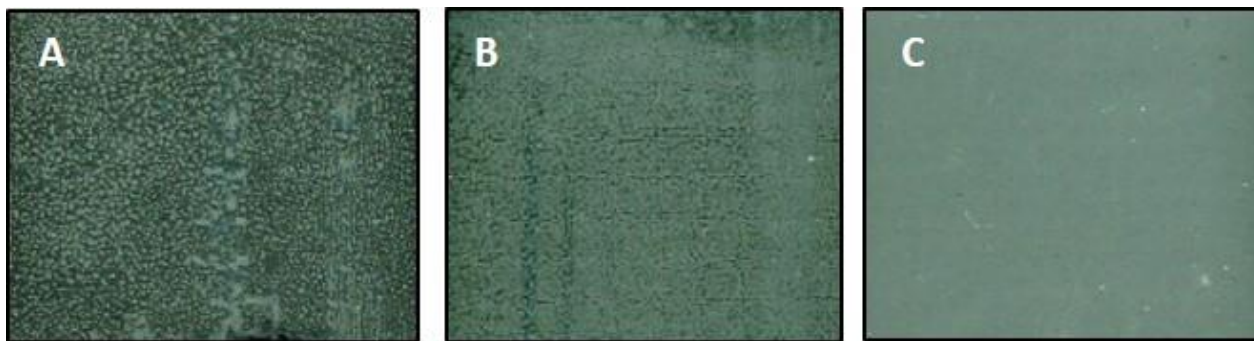


Figure S2. Effect of increasing organic solvent composition on the homogeneity of the resulting printing output, where A) 20% MeOH, B) 50% MeOH, and C) 70% MeOH.

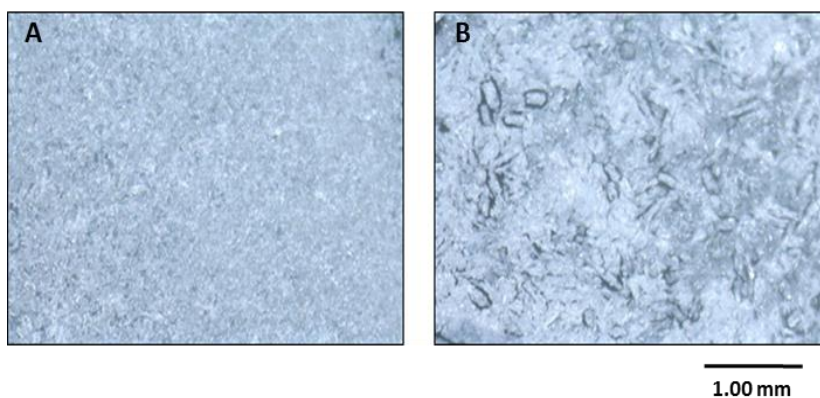


Figure S3. Digital microscope camera images of matrix crystals after 5 printing cycles of ink solution (DHB = 120 mg mL^{-1} in 70% MeOH, 0.1% TFA). A) Pre-heating of the glass slide during 5s on a hot plate at 50°C before each printing cycle, and B) at room temperature.

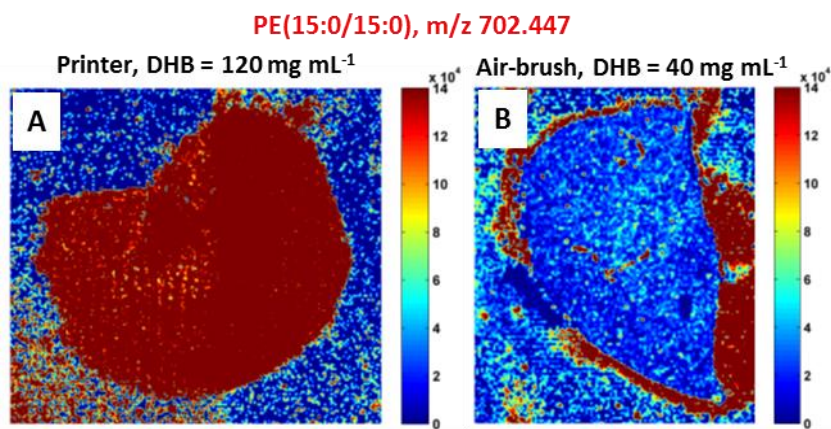


Figure S4. Effect of increasing DHB concentration on the ionization of the internal standard. Extracted ion images of $[M+K]^+$ of the PE(15:0/15:0) internal standard at m/z 702.447 obtained for (A): inkjet printer at 120 mg mL^{-1} DHB, and (B): air-brush nebulizer at 40 mg mL^{-1} DHB. Both tissues present 30 printing cycles and the same internal standard concentration.

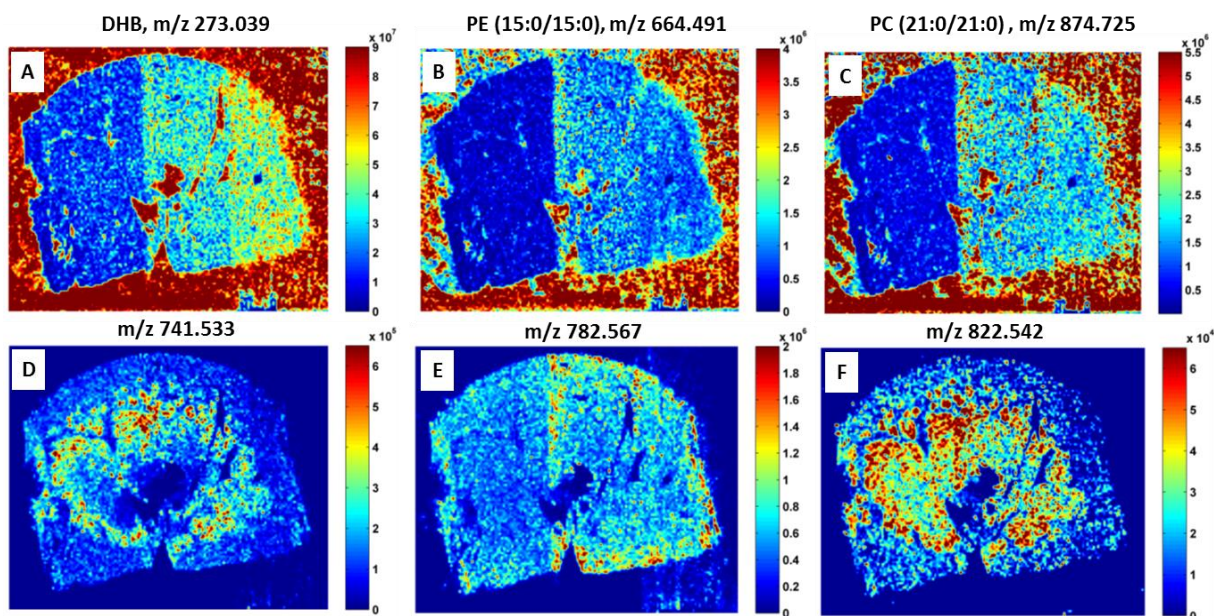


Figure S5. The effect of the number of printing cycles on the extracted ion images of a kidney tissue section with 20 printing cycles on the left side and 30 on the right side. (A) DHB, $[2M-2H_2O]^+$ at m/z 273.039. (B) $[M+H]^+$ adduct of the PE (15:0/15:0) internal standard at m/z 664.491. (C) $[M+H]^+$ adduct of the PC (21:0/21:0) internal standard at m/z 874.725. (D-F) Tissue lipids at m/z 741.533, 782.567, and 822.542, respectively.

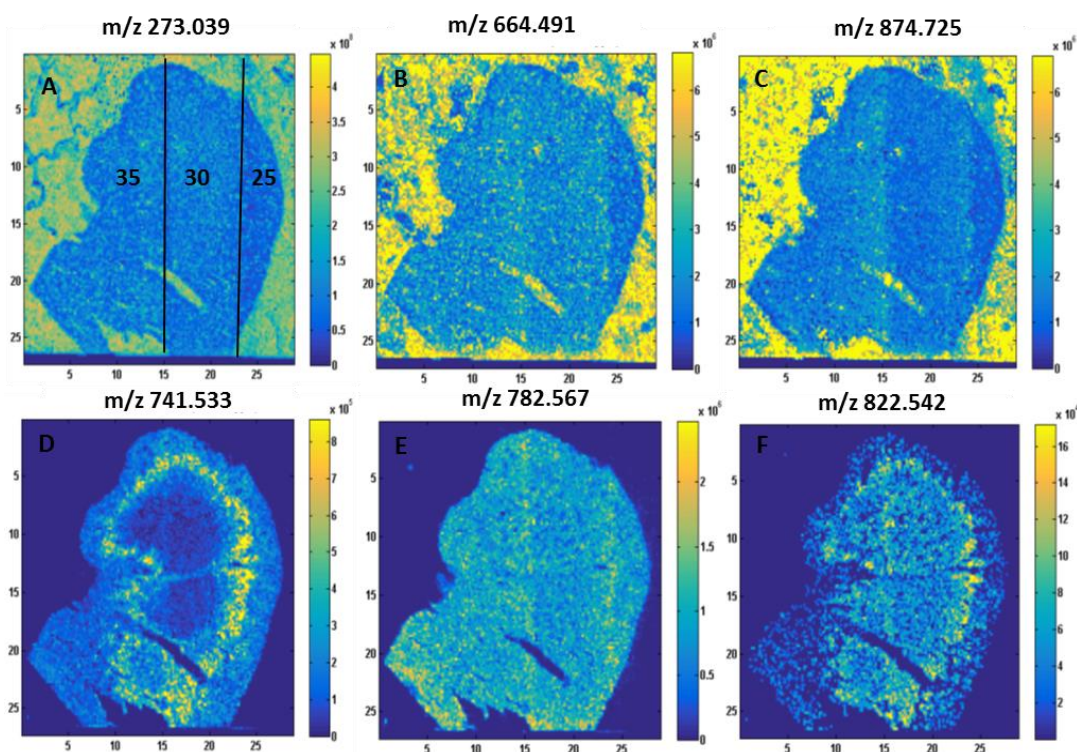


Figure S6. Kidney tissue section with 35 printing cycles on the left side, 30 on the middle part, and 25 on the right side. No enhancement of matrix and internal standard signal upon printing more than 30 cycles (A to C). (A) DHB, $[2M-2H_2O]^+$ (m/z 273.039). (B) $[M+H]^+$ adduct of the PE (15:0/15:0) internal standard (m/z 664.487). (C) $[M+H]^+$ adduct of the PC (21:0/21:0) internal standard (m/z 874.725). (D to F) Tissue lipids showing stable ionization at m/z 741.528, m/z 782.565, and m/z 822.542, respectively.

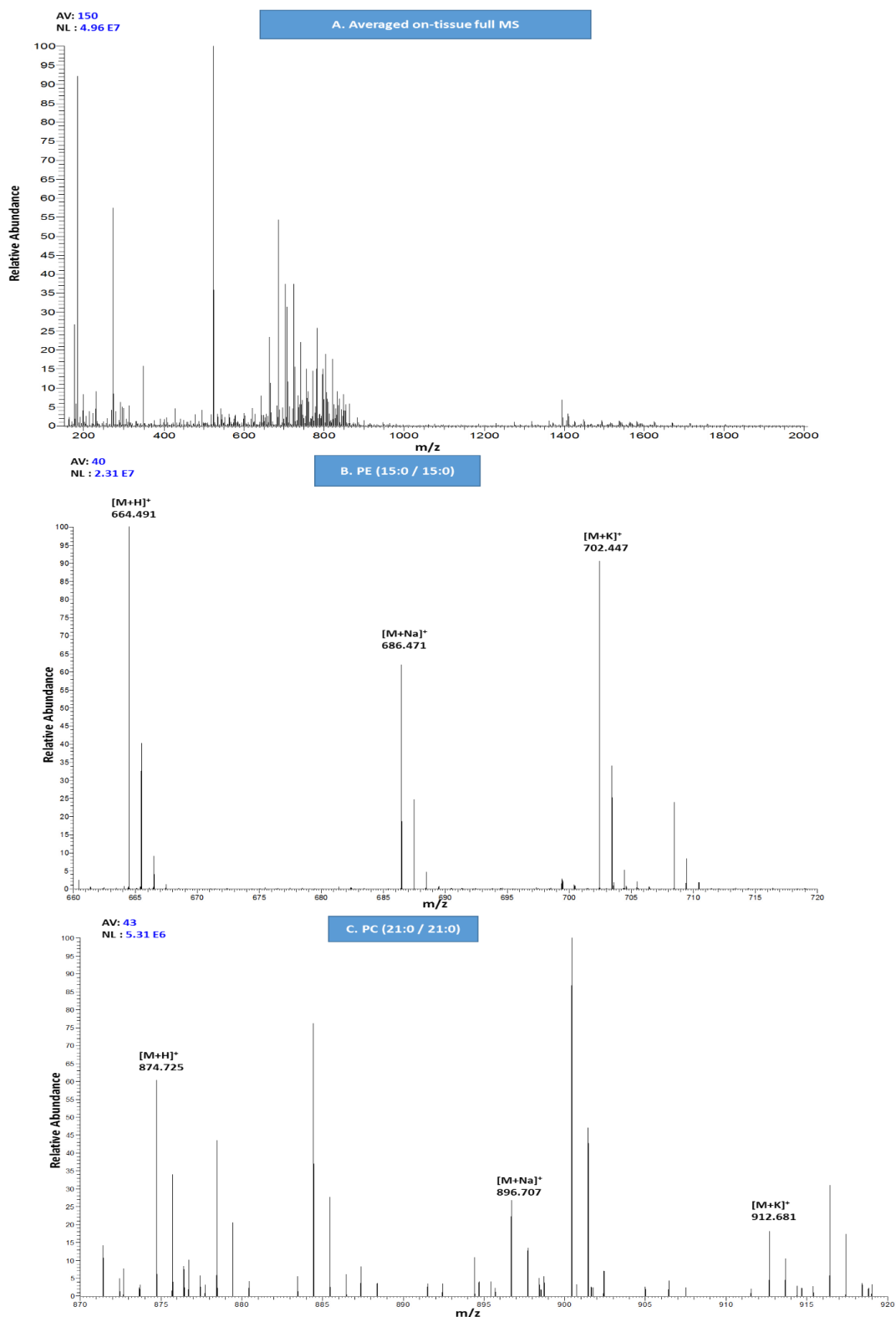


Figure S7. (A) Mass spectrum illustrates the spectral quality of a kidney tissue section printed with 30 cycles of matrix-internal standards mixture, tissue lipids are observed in the m/z range from 700-900. (B) H^+ , Na^+ and K^+ adducts of the lipidic internal standard PE (15:0/15:0) at m/z 664.491, m/z 686.470 and m/z 702.447, respectively. (C) H^+ (m/z 874.725), Na^+ (m/z 896.707), and K^+ (m/z 912.680) adducts of the lipidic internal standard PC (21:0/21:0).

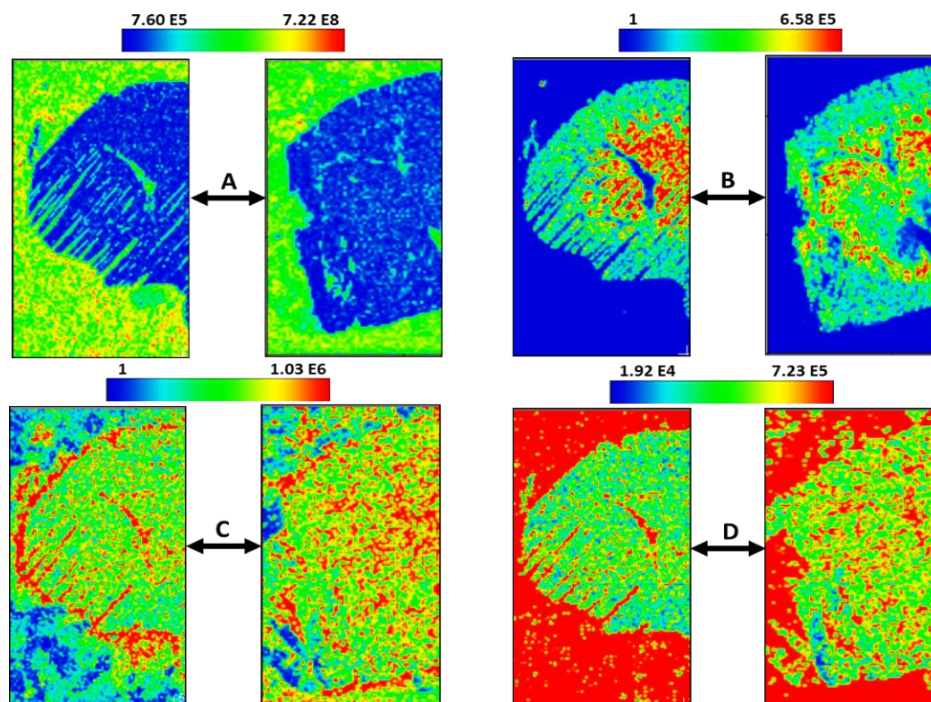


Figure S8. Reproducibility of MALDI images is demonstrated in two kidney tissue sections printed according to optimized parameters. (A) DHB signal at m/z 273.039. (B) Endogenous lipid at m/z 741.533. (C) $[M+K]^+$ of the PE (15:0/21:15:0) internal standard at m/z 702.447. (D) $[M+Na]^+$ of the PC (21:0/21:0) internal standard at m/z 896.707.

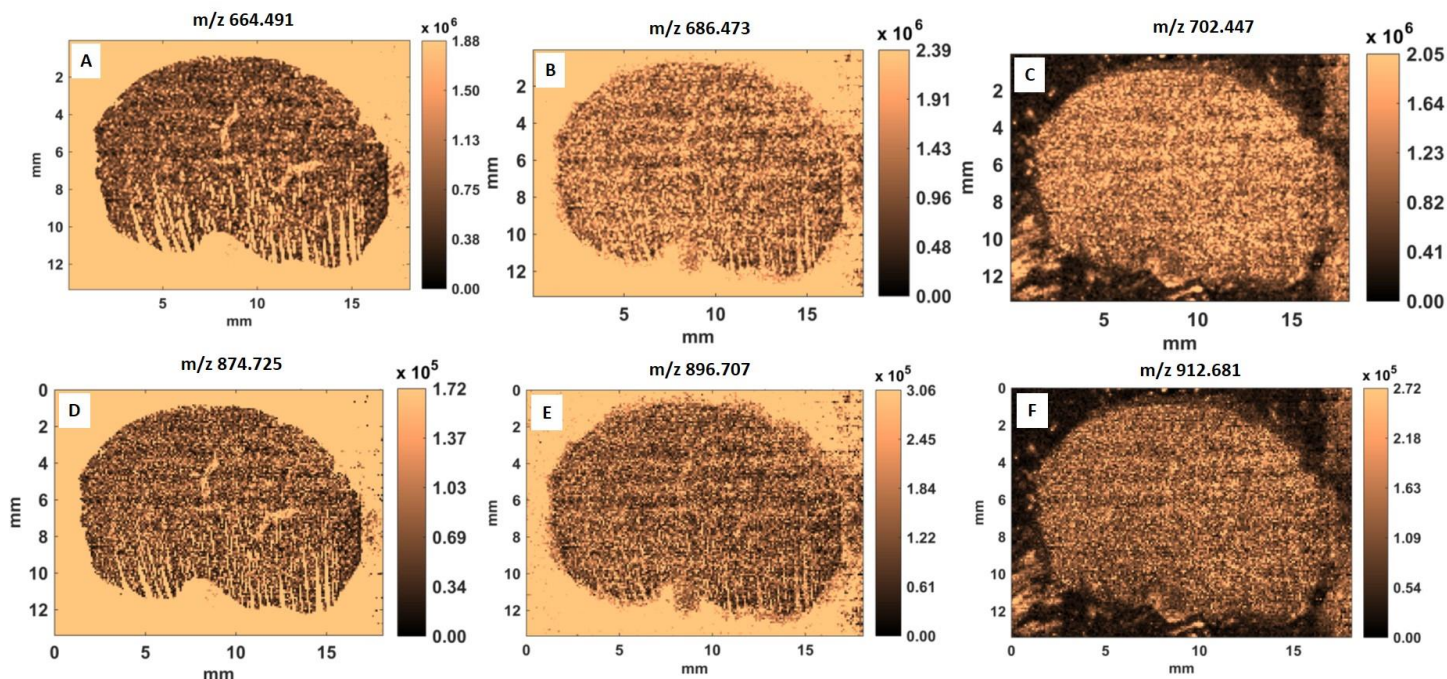


Figure S9. (A-C) Ion extracted images showing on-tissue distribution of H^+ , Na^+ , and K^+ adducts of IS PE (15:0/15:0) at m/z 664.491, 686.473, and 702.447, respectively. (D-F) Ion images showing on-tissue distribution of H^+ , Na^+ and K^+ adducts of IS PC (21:0/21:0) at m/z 874.725, m/z 896.707 and m/z 912.681, respectively.

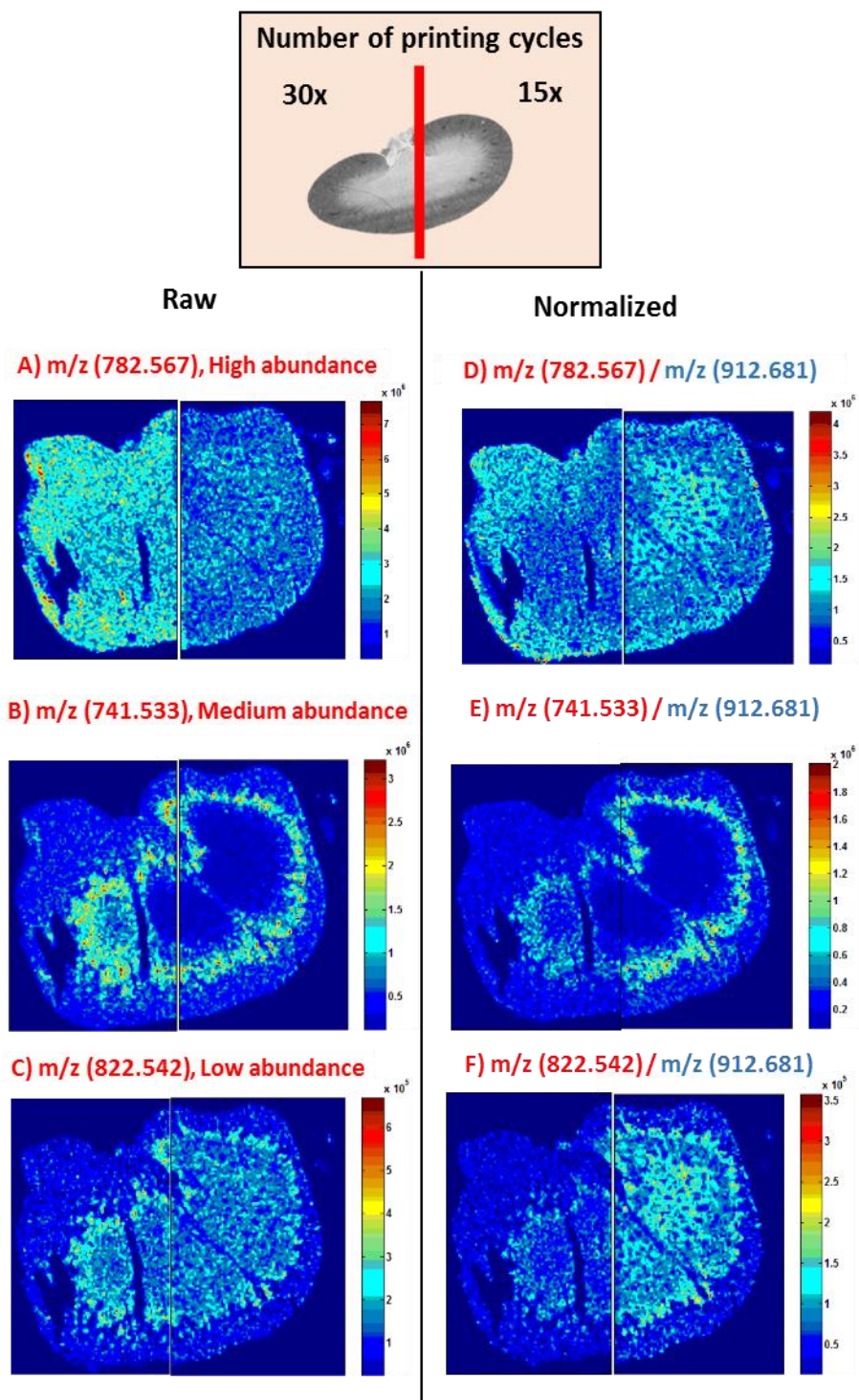


Figure S10. Color codes illustrate the effect of a proportional variation of matrix and internal standards amounts. Endogenous lipids with high, medium and low abundance are shown in panels A, B and C, respectively. Panels D, E and F show the same m/z images corrected by $M+K^+$ of PC internal standard, m/z 912.681.

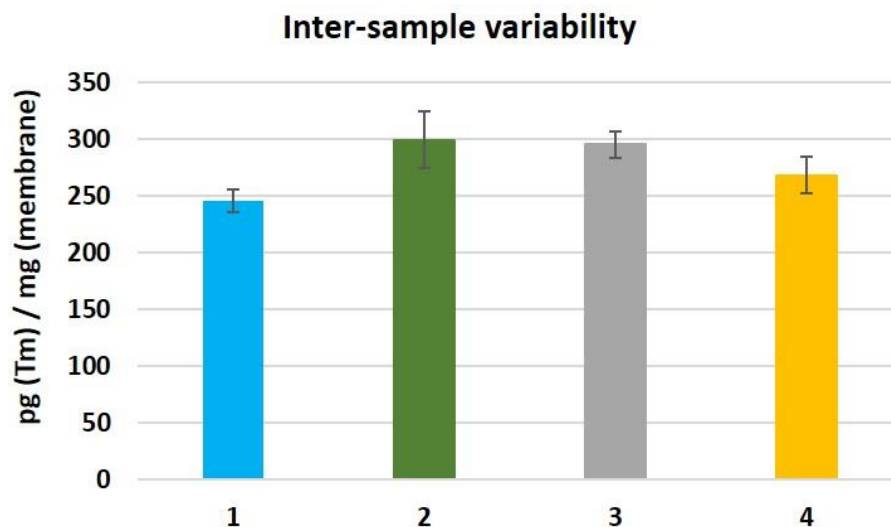


Figure S11. Metal amounts in mineralized membranes printed simultaneously with the tissues. Nitrocellulose membrane from each printing experiment weighed approx. 2-4 mg. Metal content in the different samples showed a mean value of 277 pg (Tm) / mg (membrane) with a RSD value of 11%. Error bars indicate the s.e.m

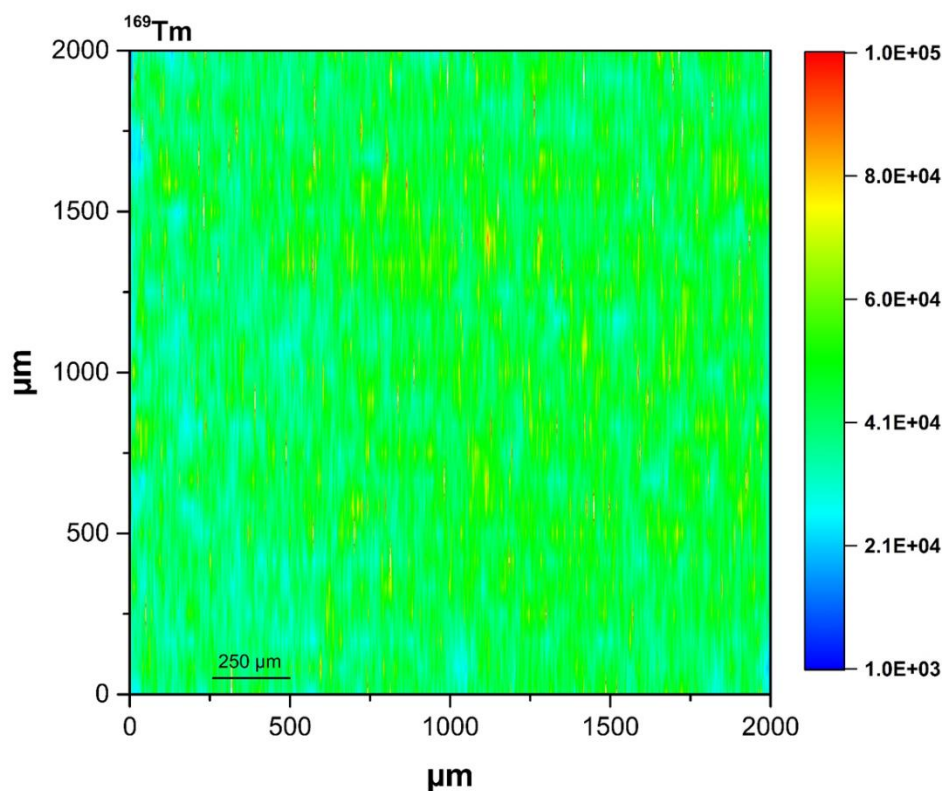


Figure S12. Intensity profile of ¹⁶⁹Tm using LA-ICP-MS of a 2 mm² area of a NC membrane, which received 30 printing cycles of the optimized matrix/internal standards mixture. RSD value of 2-4% was found between the different ablated lines within the membrane.

where the mean value in each sample is calculated using 3 replicates.

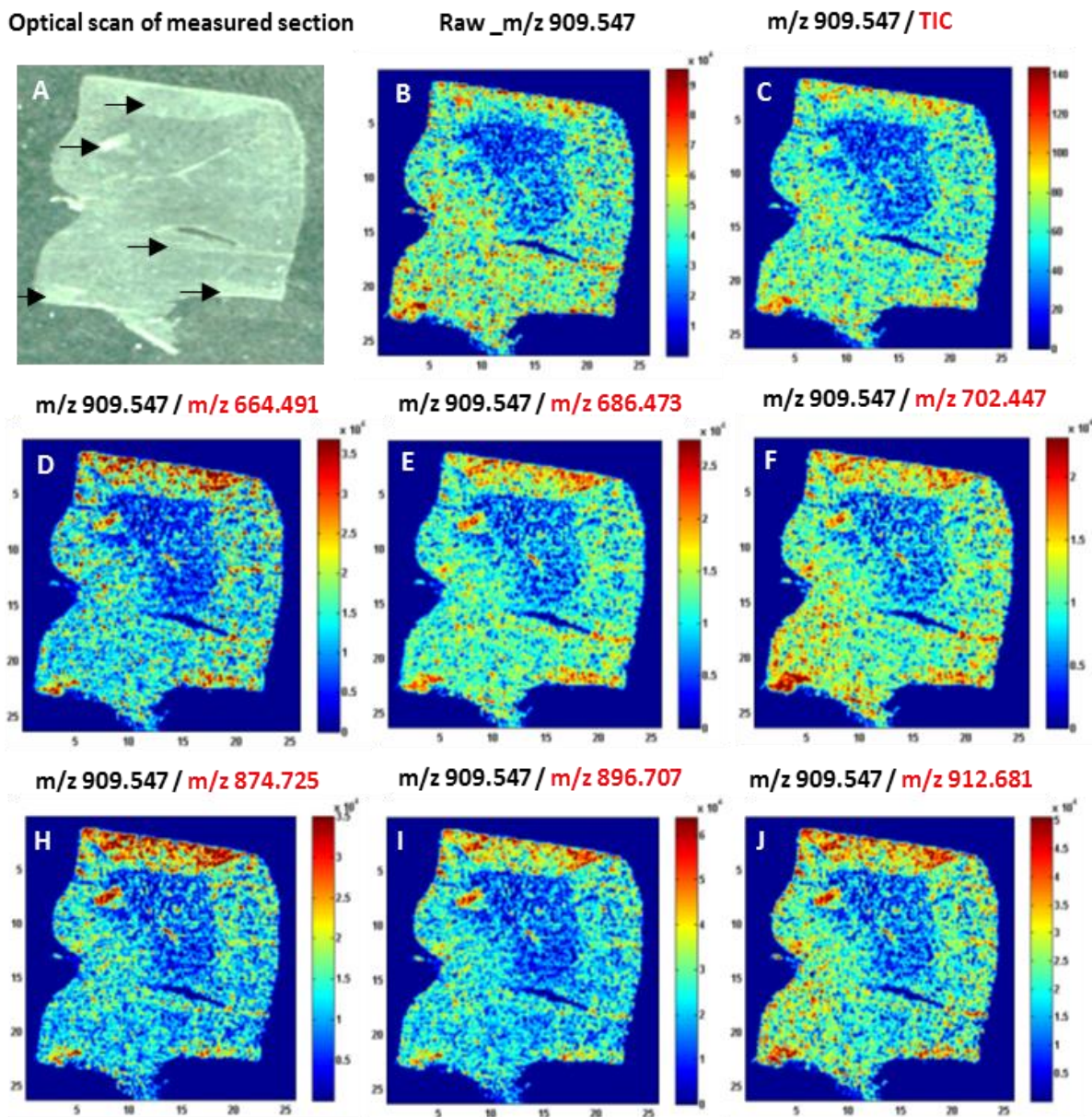


Figure S13. Improved reflection of tissue irregularities observed in internal standard normalized MALDI images for m/z 909.547 (PI(38:4), $[M+Na]^+$). (A) Optical scan of the measured tissue. (B) Raw MALDI image of m/z 909.547. (C) TIC-normalized image. (D to F) Normalized images of m/z 909.547 to $[M+H]^+$, $[M+Na]^+$ and $[M+K]^+$ of PE (15:0/15:0) at m/z 664.491, m/z 686.473, and m/z 702.447, respectively. (G to I) Normalized images of m/z 909.547 to $[M+H]^+$, $[M+Na]^+$ and $[M+K]^+$ of PC(21:0/21:0) at m/z 874.725, m/z 896.707 and m/z 912.681, respectively.

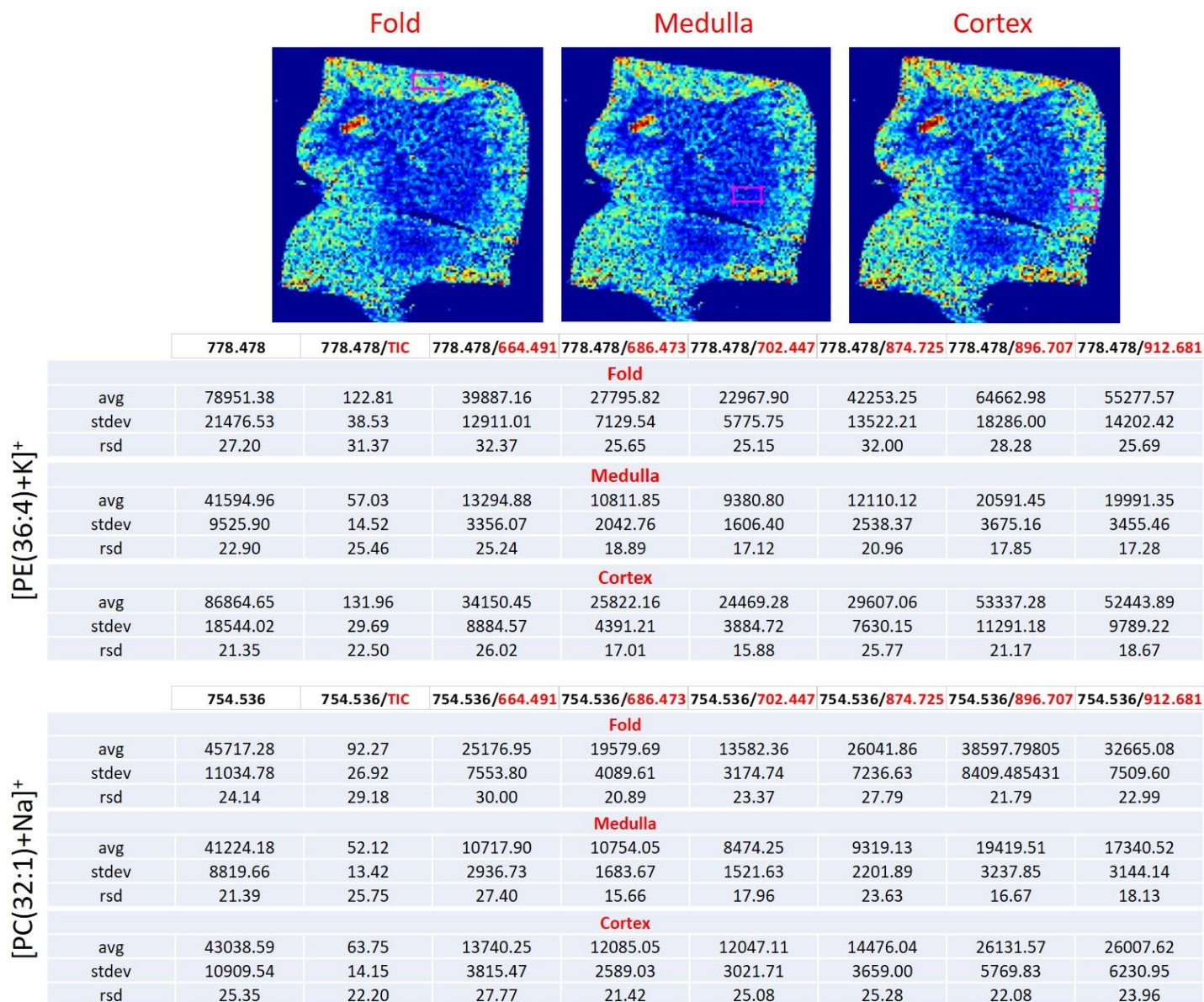


Figure S14. Mean relative intensity calculated in different ROIs (regions of interest) in the tissue section for m/z 778.478 and m/z 754.536 (marked in magenta: Upper, Middle and Right, each ROI contains approx. 100 pixels). The tables show average, standard deviation and relative standard deviation for non-normalized, TIC-normalized and different internal standards adducts-normalized intensity at m/z 664.491, m/z 686.473, m/z 702.447, m/z 874.725, m/z 896.707 and m/z 912.681, corresponding to $[M+H]^+$, $[M+Na]^+$, $[M+K]^+$ for PE(15:0/15:0) and PC(21:0/21:0), respectively.

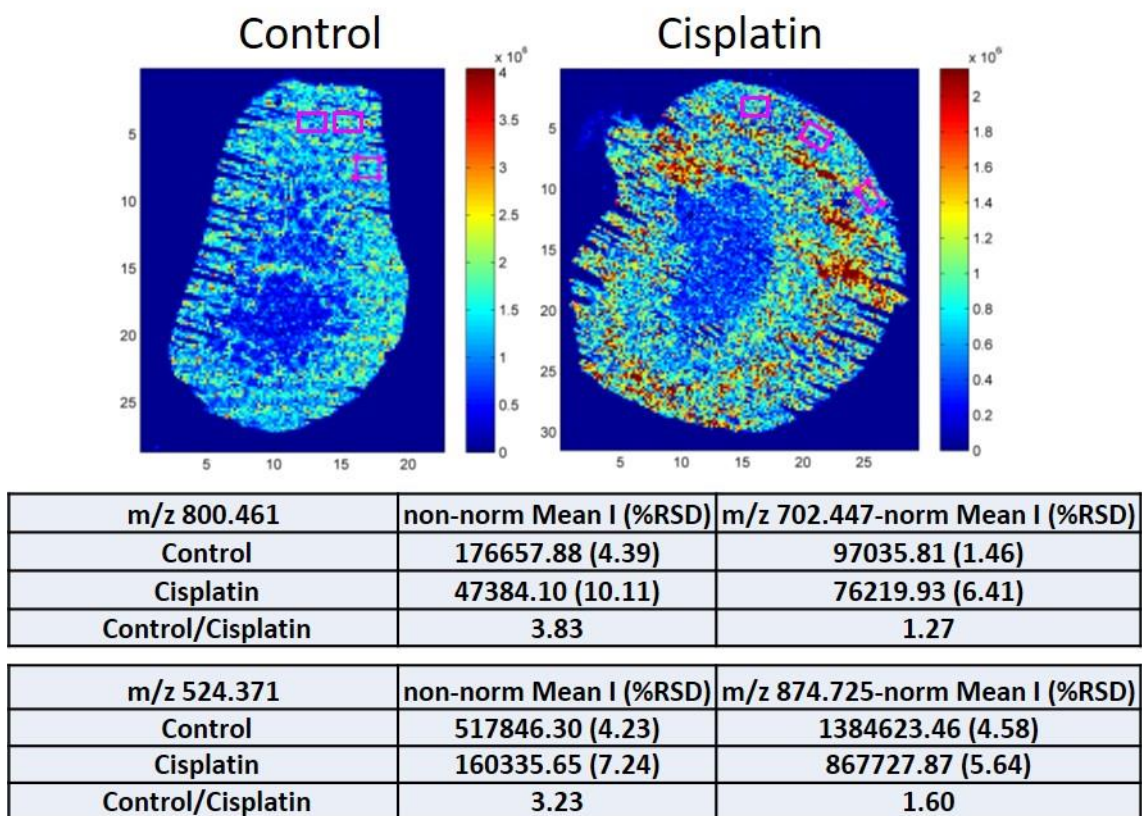


Figure S15. Raw and IS-normalized mean intensity and %RSD over 3 ROIs (highlighted in the MALDI images in magenta, each ROI has 75 pixel) in the cortex of control and cisplatin-treated tissues for m/z 524.371 and m/z 800.461.